Drug and Alcohol Dependence 170 (2017) 43–50

Contents lists available at ScienceDirect

Drug and Alcohol Dependence

journal homepage: www.elsevier.com/locate/drugalcdep

Full length article

Evaluation of TSPO PET imaging, a marker of glial activation, to study the neuroimmune footprints of morphine exposure and withdrawal

Sylvain Auvity[a,b,c,d], Sébastien Goutal[d], Benoît Thézé[d], Catarina Chaves[a,b,c,e], Benoît Hosten[a,b,c,f], Bertrand Kuhnast[d], Wadad Saba[d], Raphaël Boisgard[d], Irène Buvat[d], Salvatore Cisternino[a,b,c,f], Nicolas Tournier[d,*]

[a] Variabilité de la Réponse aux Psychotropes, INSERM U1144, Paris F-75006, France
[b] Université Paris Descartes, UMR-S 1144, Paris F-75006, France
[c] Université Paris Diderot, UMR-S 1144, Paris F-75013, France
[d] Imagerie Moléculaire In Vivo, IMIV, CEA, Inserm, CNRS, Univ. Paris-Sud, Université Paris Saclay, CEA-SHFJ, Orsay F-91401, France
[e] REQUIMTE, Laboratório de Toxicologia, Departamento de Ciências Biológicas, Faculdade de Farmácia, Universidade do Porto, Porto, Portugal
[f] Assistance publique hôpitaux de Paris, AP-HP, Paris F-75004, France

ARTICLE INFO

Article history:
Received 10 August 2016
Received in revised form 12 October 2016
Accepted 29 October 2016
Available online 8 November 2016

Keywords:
Microglia
Opioid
Addiction
Tolerance
DPA-714
Neuroinflammation

ABSTRACT

Introduction: A growing area of research suggests that neuroimmunity may impact the pharmacology of opioids. Microglia is a key component of the brain immunity. Preclinical and clinical studies have demonstrated that microglial modulators may improve morphine-induced analgesia and prevent the development of tolerance and dependence. Positron emission tomography (PET) using translocator protein 18 kDa (TSPO) radioligand is a clinically validated strategy for the non-invasive detection of microglial activation. We hypothesized that TSPO PET imaging may be used to study the neuroimmune component of opioid tolerance and withdrawal.

Methods: Healthy rats (n = 6 in each group) received either saline or escalating doses of morphine (10–40 mg/kg) on five days to achieve tolerance and a withdrawal syndrome after morphine discontinuation. MicroPET imaging with [^{18}F]DPA-714 was performed 60 h after morphine withdrawal. Kinetic modeling was performed to estimate [^{18}F]DPA-714 volume of distribution (V_T) in several brain regions using dynamic PET images and corresponding metabolite-corrected input functions. Immunohistochemistry (IHC) experiments on striatal brain slices were performed to assess the expression of glial markers (Iba1, GFAP and CD68) during 14 days after morphine discontinuation.

Results: The baseline binding of [^{18}F]DPA-714 to the brain ($V_T = 0.086 \pm 0.009$ mL cm^{-3}) was not increased by morphine exposure and withdrawal ($V_T = 0.079 \pm 0.010$ mL cm^{-3}) indicating the absence of TSPO overexpression, even at the regional level. Accordingly, expression of glial markers did not increase after morphine discontinuation.

Conclusions: Morphine tolerance and withdrawal did not detectably activate microglia and had no impact on [^{18}F]DPA-714 brain kinetics in vivo.

1. Introduction

Morphine is a widely used analgesic drug against acute and chronic pain (Trescot et al., 2008). A major specificity of morphine pharmacology relies on its high potency to induce tolerance. Morphine may also create dependence, a psychological and physical need of drug abuse to avoid the appearance of a withdrawal syndrome (Nielsen and Kreek, 2012). The central nervous system (CNS) footprint of opioid pharmacology has been mainly investigated through the lens of neuronal pathways, especially the opioid systems (Koob and Volkow, 2010).

The suppressive impact of morphine exposure and withdrawal on peripheral innate and adaptive immunity is well described and is often correlated to the increased prevalence of opportunistic infective agents in opioid abusers (Roy et al., 2011). In the brain, it was shown that immunity may contribute to opioid neuropharmacology, as illustrated with opioid-induced Toll-like receptor 4 (TLR4) inflammatory pathways and the release of pro-inflammatory cytokines (Hutchinson et al., 2011). Conversely, it

* Corresponding author at: Laboratoire Imagerie Moléculaire In Vivo (IMIV), CEA, Service Hospitalier Frédéric Joliot, 4 Place du General Leclerc, 91401 Orsay, France.
E-mail address: nicolas.tournier@cea.fr (N. Tournier).

http://dx.doi.org/10.1016/j.drugalcdep.2016.10.037
0376-8716/

was shown that chronic morphine exposure suppresses the innate immunity of microglia in the brain (Qiu et al., 2015), which may balance its intrinsic pro- inflammatory effects in vivo.

Microglial cells are key components of innate immunity in the brain (Saijo and Glass, 2011). Resting microglial cells exert active surveillance of their environment and switch to an activated phenotype in the presence of a variety of deleterious stimuli like those involving TLR4 interactions (Mosser and Edwards, 2008). Microglial responsiveness places these cells as diagnostic markers of inflammation onset or progression in CNS diseases (Perry et al., 2010). It was proposed that microglia may be a key component of the impact of morphine exposure to the brain (Watkins et al., 2005). Microglia modulates some of the effects of opioids (Hutchinson et al., 2007) including their pain relieving properties (Watkins et al., 2009) as well as their reward and dependence potency (Coller and Hutchinson, 2012; Hutchinson et al., 2012). Recent clinical trials suggest that ibudilast, a modulator of microglial functions, may improve the efficacy and tolerance profile of opioids during the management of chronic pain and was recently shown to decrease some subjective ratings of opioid withdrawal symptoms (Cooper et al., 2015; Johnson et al., 2015).

The immune component of opioid pharmacology suggests that glial cell activation may also represent a relevant pathophysiological biomarker of the development of addiction and its extinction, and thus provide a potential monitoring biomarker for the management of opioid abuse (Hutchinson and Watkins, 2014). The most advanced approach allowing for the non-invasive investigation of glial activation in human is positron emission tomography (PET) imaging using radiolabelled ligands of the translocator protein–18 kDa (TSPO). TSPO is mainly located on the outer mitochondrial membrane of several cells and involved in cholesterol and steroidogenesis. Baseline TSPO expression in the brain under physiological conditions contrasts with measurable TSPO overexpression detected in several neuroinflammatory diseases (Corcia et al., 2012). [^{18}F]DPA-714, a TSPO radioligand, was successfully used to visualize activated microglia in preclinical models of traumatic brain injury (Wang et al., 2014a), epilepsy (Harhausen et al., 2013) or stroke (Wang et al., 2014b). [^{18}F]DPA-714 has reached the clinical status, allowing for the clinical translation of preclinical findings (Arlicot et al., 2012; Lavisse et al., 2015).

In the present study, we investigated the potency of TSPO PET imaging using [^{18}F]DPA-714 to detect glial cell activation in a validated rat model of chronic morphine exposure and withdrawal (Desjardins et al., 2008). We used immunohistochemistry (IHC) with selected glial cell biomarkers that were shown to corroborate [^{18}F]DPA-714 PET signal in order to establish the kinetic profile of glial cell activation after morphine discontinuation and the development of a withdrawal syndrome.

2. Material and methods

2.1. Animals and drugs

Pathogen-free male Sprague Dawley rats (250–350 g) were purchased from Charles River (St Germain sur l'arbresle, France) and housed in standard conditions with an access to food and water *ad libitum*. Rats were maintained in a 12h-dark/light cycle. Animals were housed for a five day adaptation period before experimentation. All experiments complied with the standards and guidelines promulgated by the European Union Council Directive (2010/63/EU) for the experimentation with laboratory animals and were approved by the ethics review committee (Paris Descartes University approval n°12-186). All efforts were made to minimize animal suffering and to use only the number of animals necessary to produce reliable scientific data. Morphine sulfate sterile solution was purchased from Aguettant (Lyon, France). Doses are reported as free base.

2.2. Animal models

We used a well described and in-house validated rat model of morphine exposure and tolerance followed by spontaneous withdrawal syndrome after morphine discontinuation (behavioral validation) (Desjardins et al., 2008). Animals were given intraperitoneal (*i.p*) morphine twice daily: 10 mg/kg on day 1, 20 mg/kg on day 2, 30 mg/kg on day 3 and 40 mg/kg on day 4 and 5 (Table 1). Control animals received an equivalent volume of sterile 0.9% sodium chloride instead of morphine solution.

MicroPET experiments were performed 60 h after the last injection of morphine to compare with previously published data using a similar model (Campbell et al., 2013).

IHC analysis was performed at different time points after morphine chronic exposure. It began just after the last injection of morphine (referenced as "day 5") and was continued on days 8, 10, 12, 15, 17 and 19. As a positive control, we performed a well characterized model of acute local neuroinflammation with positive TSPO expression, developed in-house for the validation of many TSPO radioligands including [^{18}F]DPA-714 (Chauveau et al., 2009). Briefly two rats were stereotactically injected 0.5 μL of (R,S)-α-amino-3-hydroxy-5-methyl-4- isoxazolopropionic acid (AMPA) (15 mM in phosphate-buffered saline; Sigma, St Quentin, France) in the right striatum using a microsyringe and micropump (UltraMicroPump II and Micro4 Controller; WPI Inc.). Rats were then decapitated 7 days after the AMPA injection and the brains were immediately frozen in isopentane maintained at −40 °C.

2.3. PET study

2.3.1. Radiochemistry. [^{18}F]DPA-714 (*N,N*-diethyl-2-(2-(4-(2-[^{18}F]fluoroethoxy)phenyl)-5,7-dimethylpyrazolo [1,5-a]pyrimidin-3-yl)acetamide) was produced on site according to slight modifications of procedures already reported (Damont et al., 2008), using a commercially available GE TRACERLab FX-FN synthesizer (Kuhnast et al., 2012). Ready-to-inject >99% radiochemically pure [^{18}F]DPA-714 formulated in 0.9% sodium chloride containing less than 10% (v/v) of ethanol was obtained with specific radioactivity at the end of the radiosynthesis ranging from 45 to 100 GBq/μmol.

2.3.2. MicroPET scans and data acquisition. Anesthesia was conducted using isoflurane in O_2, 4% for induction and 1.5–2.5% thereafter. The tail vein was catheterized. Rats were positioned with their head in the center of the field of view. Dynamic PET data acquisition was performed using a Siemens INVEON (Siemens Medical Solutions, St Denis, France) dedicated to small animal with a spatial resolution of 1.4 mm in reconstructed images. A Fourier rebinning and an OSEM 2D reconstruction method was implemented. Animals were kept normothermic thanks to a heating blanket. Each animal was injected with 32.60 ± 7.22 MBq and a dynamic acquisition was performed during 68 min, beginning at the time of injection. The [^{18}F]DPA-714 images were sorted into 24 frames ranging from 0.5 to 10 min each. A brain template (Schiffer et al., 2006) was applied to each image to delineate different volumes of interest (VOI) on the accumbens nucleus, amygdala, striatum, hippocampus, hypothalamus, thalamus, midbrain, cortex and whole brain.

2.3.3. Arterial input function. Additional animals were used to measure [^{18}F]DPA-714 metabolite-corrected arterial input function in parallel conditions. Blood samples (200 μL) were collected at

Table 1
Protocol of morphine exposure and spontaneous withdrawal. Morphine was injected intraperitoneally (*i.p*) using escalating doses of morphine: 10 mg/kg on day 1, 20 mg/kg on day 2, 30 mg/kg on day 3 and 40 mg/kg on day 4 and 5, twice daily. Days 6 and 7 were free from injection to allow for the morphine withdrawal syndrome to appear. Animals underwent microPET imaging 60 h after the last injection of morphine and were sacrificed immediately after. AM and PM indicate morning and evening injections, respectively. Control rats received equivalent volumes of 0.9% sodium chloride instead of morphine.

		Day 1 (mg/kg)	Day 2 (mg/kg)	Day 3 (mg/kg)	Day 4 (mg/kg)	Day 5 (mg/kg)	Day 6 (mg/kg)	Day 7 –	Day 8 –
Morphine injections	AM	10	20	30	40	40	–	–	PET
	PM	10	20	30	40	40	–	–	

selected times from the femoral artery to establish total radioactivity kinetics in arterial plasma. Samples were centrifuged (3 min, 2054*g*, 4 °C) and radioactivity in cell-free plasma (100 μL) was counted. Additional samples (500 μL) were withdrawn at 10, 20, 40 and 60 min after injection to determine the fraction of parent [^{18}F]DPA-714 in plasma using a validated solid phase extraction method (Peyronneau et al., 2013). The fraction of parent [^{18}F]DPA-714 *versus* time was fitted using a 1-exponential decay equation and applied to the total radioactivity kinetics to estimate the metabolite-corrected arterial input function of [^{18}F]DPA-714 in the rat model of morphine exposure and withdrawal (60 h after morphine withdrawal, n = 3) and in control animals (saline, n = 3).

2.3.4. PET data analysis. Radioactivity in each brain VOI was expressed as a percentage of injected dose (% I.D.cm^{-3}). Data are presented as time-activity curves (TACs) in each VOI. Kinetic modelling was performed using Pmod® software (version 3.6; Switzerland). [^{18}F]DPA-714 volume of distribution (V_T, mL cm^{-3}) in each brain region was estimated using the Logan plot analysis, taking the metabolite corrected arterial input function into account.

2.4. Immunohistochemistry

Expression of biomarkers of glial cell activation was assessed using IHC on striatal brain slices during 14-days after morphine discontinuation. This invasive approach was performed in order to explain the PET data and provide temporal and quantitative information regarding glial response during chronic morphine exposure and withdrawal. Indeed, it was shown that ionized calcium-binding adapter molecule 1 (Iba1), Cluster of Differentiation 68 (CD68), a lysosomal protein, and glial fibrillary acidic protein (GFAP) expression are up-regulated and corroborate [^{18}F]DPA-714 binding to the brain (Lavisse et al., 2012).

Extemporaneously collected and non-perfused rat brains were snap frozen in isopentane, maintained at −40 °C and stored at −80 °C until IHC experiments. For immunohistochemical labelling, 10 μm-thick tissue sections retrieved in the striatum area were post-fixed in buffered paraformaldehyde (4%, 10 min, room temperature (R/T)), followed by ammonium chloride solution (50 mM, 5 min, R/T). Tissue permeabilization was performed in methanol-acetone solution (1:1, 5 min, −20 °C) and triton X100 solution (0.1%, 5 min, R/T). Non-specific binding sites were blocked with 5% bovine serum albumin (BSA, Sigma) and 0.5% Tween20 (Sigma). Slides were then incubated (1 h, R/T) with the following primary antibodies: chicken anti-GFAP (1:500, ab4674, Abcam, Paris, France), mouse anti-CD68 (1:100, MCA341R, Serotec, Colmar, France) or goat anti-Iba1 (1:100, ab5076, Abcam). After phosphate buffer saline (PBS, Sigma) washes, secondary detection reagents were respectively: AF647-goat anti chicken (1:1000, A21449, Life Technologies), AF594-goat anti mouse (1:1000, A11032, Life Technologies) or AF647-donkey anti goat (1:1000, A21447, Life Technologies). Slides were mounted with ProLong Gold Antifade containing 4′,6′- diamidino-2-phenylindole (DAPI, Life technologies).

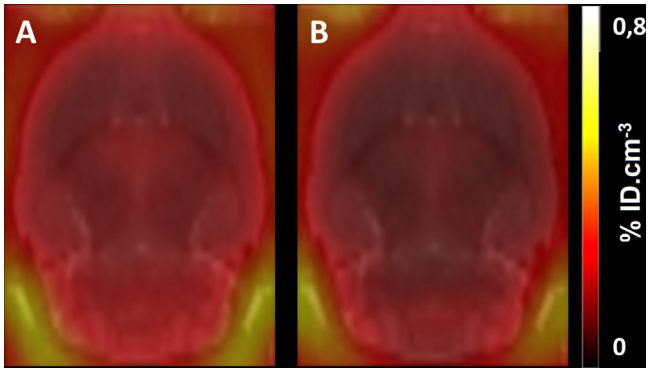

Fig. 1. Representative [^{18}F]DPA-714 brain PET images obtained in each experimental condition. Data are represented as summed images (20–68 min), for the control (A) and the morphine-treated group (B). PET images were smoothed and overlaid to a coregistered MRI template.

2.5. Microscopy image acquisition and analysis method

The fluorescently labelled tissue sections were scanned at resolution 0.97 μm per pixel using an AxiObserver Z1 (Zeiss, Germany). Striatal slides from two different rat brains were analyzed for each time point of the kinetic of biomarker expression. The number of digitalized slides per rat was n = 3 for each biomarker. Image analysis was automated using macros implemented in the Image J software (NIH, Bethesda, MD, USA). Briefly, background fluorescence variability was corrected by inter-slide global intensity normalization, followed by intra-slide unidirectional filtering for local minimum intensity normalization. In the case of the Iba1 labelling, as a slight signal was unexpectedly present in the some cell nuclei, the DAPI staining was used as a mask, and only the cytoplasmic Iba1 signal was considered for quantification. After global constant image thresholding, the expression was computed as the ratio of the CD68$^+$, Iba1$^+$ or GFAP$^+$ surface area (in pixels) to the DAPI$^+$ surface area (in pixels).

2.6. Statistical analysis

All data are represented as mean ± SD. For PET data, statistical analysis was performed using R version 3.1.2. V_Ts in each VOI were compared using a two-way ANOVA analysis. Treatment and anatomical regions were defined as explanatory variables (residuals were normally distributed and homogeneous). For IHC statistical analysis, one way ANOVA followed by Bonferroni *post hoc* tests were performed. The level of significance for all hypotheses was set at $p < 0.05$.

3. Results

3.1. PET study

PET images confirmed the low baseline uptake of [^{18}F]DPA-714 in the brain (Fig. 1). The brain distribution was not visually influenced by morphine exposure and withdrawal (Fig. 1). Rep-

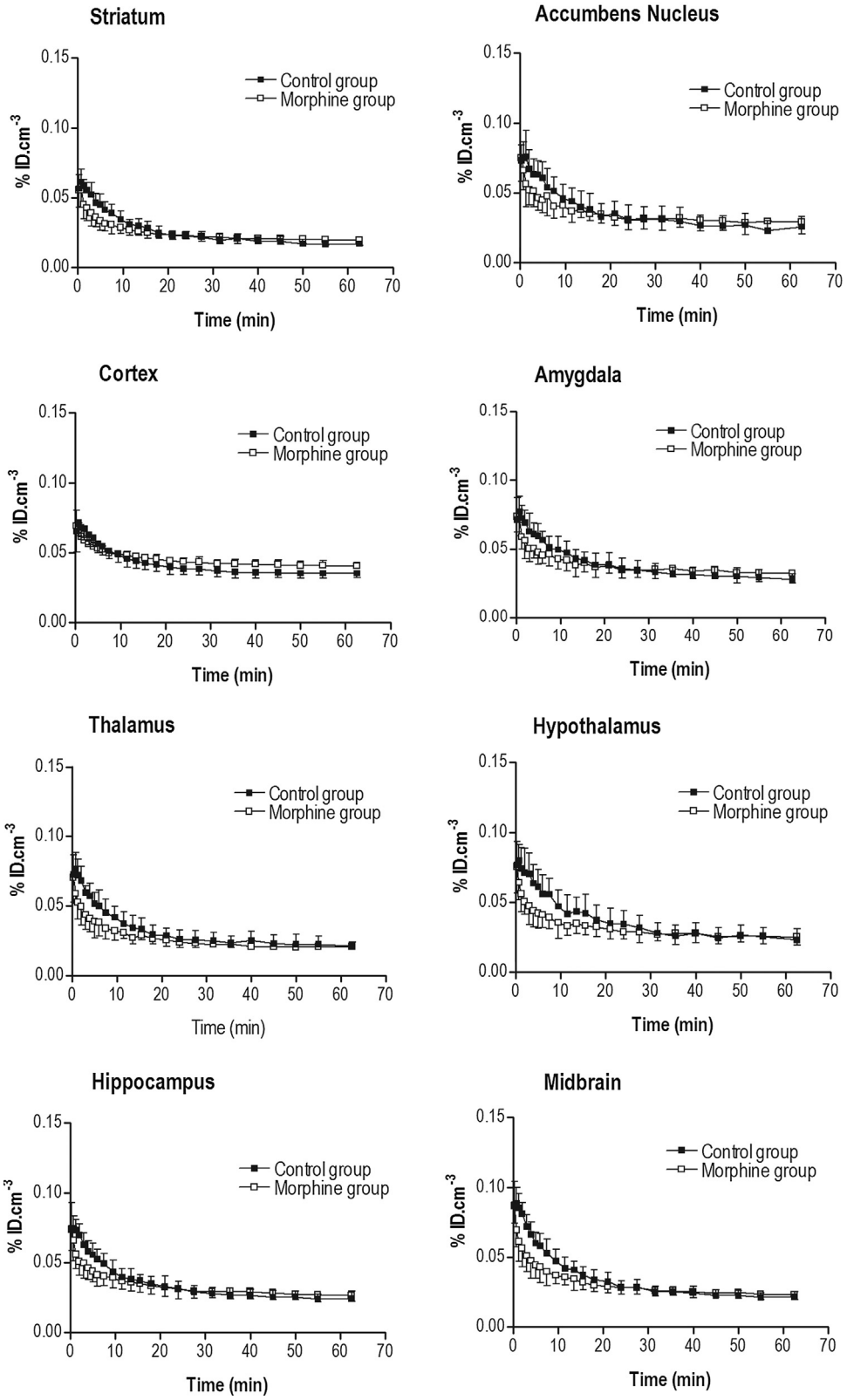

Fig. 2. [^{18}F]DPA-714 brain kinetics. Regional [^{18}F]DPA-714 time activity curves (TACs) obtained in control and morphine-treated animals are shown as a mean percentage ± SD of injected dose (% ID cm^{-3}, n = 6) *versus* time (min) in selected brain regions.

resentative TACs extracted from each VOI are shown in Fig. 2. Radioactivity reached an equilibrium 30 min after [^{18}F]DPA-714 injection in all brain regions (Fig. 2). [^{18}F]DPA-714 metabolism and plasma kinetics were similar, suggesting negligible impact of morphine exposure and withdrawal on [^{18}F]DPA-714 plasma clearance and metabolism (Fig. 3). Differences in estimated [^{18}F]DPA-714 volume of distribution (V_T) in the brain of control ($V_T = 0.086 \pm 0.009$ mL cm^{-3}) and the morphine-treated animals

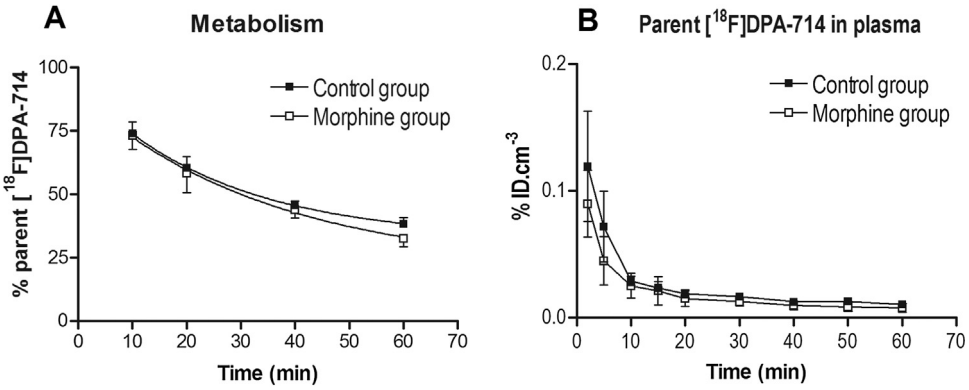

Fig. 3. [^{18}F]DPA-714 metabolism and plasma kinetics. The percentage of parent (unmetabolized) [^{18}F]DPA-714 in arterial plasma *versus* time is shown in A. The corresponding metabolite-corrected arterial input function of [^{18}F]DPA-714 from 0 to 60 min is shown in B. Data are shown as mean ± S.D (n = 3) in both the control and the morphine-treated groups.

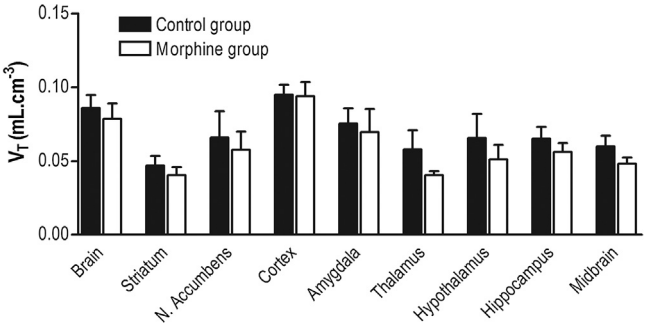

Fig. 4. [^{18}F]DPA-714 volume of distribution in selected brain regions. Kinetic modelling of the regional brain kinetics [^{18}F]DPA-714 was performed for each animal using the Logan Plot analysis and the corresponding mean parent [^{18}F]DPA-714 plasma kinetics as an input function. Reported data are means of the total volume of distribution (V_T, mL cm^{-3}) in the whole brain (brain), striatum, nucleus accumbens (N. accumbens, amygdala, hippocampus, hypothalamus, thalamus, midbrain and cortex in both the control (black column) and morphine (white column) groups (n = 6 in each group). Data are presented as mean ± SD for each region. Differences in regional V_Ts were shown not statistically significant.

($V_T = 0.079 \pm 0.010$ mL cm^{-3}) were not statistically significant. The same result was obtained all brain regions, indicating the absence of regional increase in [^{18}F]DPA-714 distribution (Fig. 4). This indicates that morphine exposure and withdrawal did not measurably impact [^{18}F]DPA-714 binding to the brain.

3.2. IHC study

In the AMPA injection model, regional overexpression of the glial activation biomarkers Iba1 and CD68 in the striatum was obvious (Fig. 5). Signal quantification confirmed this result with higher expression of Iba1 and CD68 in the AMPA group (Fig. 6). Interestingly, we found no overexpression of GFAP, suggesting minor contribution of astrocytes compared to microglia in this model.

Expressions of Iba1, CD68 and GFAP were not influenced by chronic morphine exposure compared to the control condition (Day 5, Fig. 5 and 6). The expression of tested biomarkers was not further increased at the withdrawal phase (Day 8, 60 h after morphine discontinuation, Fig. 5 and 6) compared to control group ($p > 0.05$) or Day 5 ($p > 0.05$). Kinetic analysis of the biomarker expression was performed during the withdrawal syndrome phase, from Day 8 to Day 19 (Figs. 5 and 6). The results suggest that the absence of detectable increase in TSPO PET signal is not due to any delay in microglial activation following morphine exposure and withdrawal.

4. Discussion

In the present study, we hypothesized that [^{18}F]DPA-714 PET imaging, as a non-invasive marker of glial cell activation, would be useful to detect and follow the brain immune footprints of morphine exposure and withdrawal. We chose an in vivo model of systemic morphine administration, in order to mimic morphine exposure and withdrawal in a context of morphine consumption or abuse. This model does not require any opioid-receptor antagonist to precipitate the withdrawal syndrome which spontaneously occurs as a result of drug intake cessation (Desjardins et al., 2008). This specificity is important since opioid antagonists like naloxone were also described as TLR4 inhibitors of glial activation (Hutchinson et al., 2008). This model was shown to produce at least withdrawal signs (Desjardins et al., 2008) and inflammatory brain responses unveiled by the expression of pro-inflammatory cytokines and chemokines (Campbell et al., 2013).

First, we explored the effect of morphine withdrawal on the brain immune system using [^{18}F]DPA-714 TSPO PET imaging. Compared with control animals, [^{18}F]DPA-714 binding to the brain of morphine exposed rats was not increased in any brain region. This indicates the absence of detectable TSPO overexpression after morphine withdrawal. To address this result, we performed a quantitative IHC methodology that was shown to corroborate [^{18}F]DPA-714 PET imaging in rats (Lavisse et al., 2012). The striatum was selected as a region of interest for IHC given its key contribution to addiction processes (Nutt et al., 2015). IHC data were compared to those obtained in a [^{18}F]DPA-714 PET-positive model of striatal glial activation.

IHC analysis started the day of morphine discontinuation (Day 5) to explore glial cell activation after chronic and systemic morphine exposure inducing tolerance, before the apparition of any withdrawal sign. Using our methodology, no increase in the expression of tested biomarkers could be detected, which contrasts with the dramatic increase in Iba1 and CD68 expression in the AMPA model (Fig. 5). GFAP expression was not either increased. Interestingly, GFAP was previously shown to be overexpressed (Song and Zhao, 2001) or not (Loram et al., 2012) in the spinal cord of different rat model of morphine tolerance but has never been investigated in the striatum to our knowledge.

Then, the expression of glial-cell activation biomarkers from the end of the 5 days of escalating exposure to morphine and up to the 14 days after the withdrawal phase was explored. Using this approach, we tested the hypothesis of i) a kinetic regulation of biomarker expression during the withdrawal phase and ii) a potential delay in glial cell activation after the appearance of withdrawal signs. Indeed, glial cell activation was shown to start 3 days after

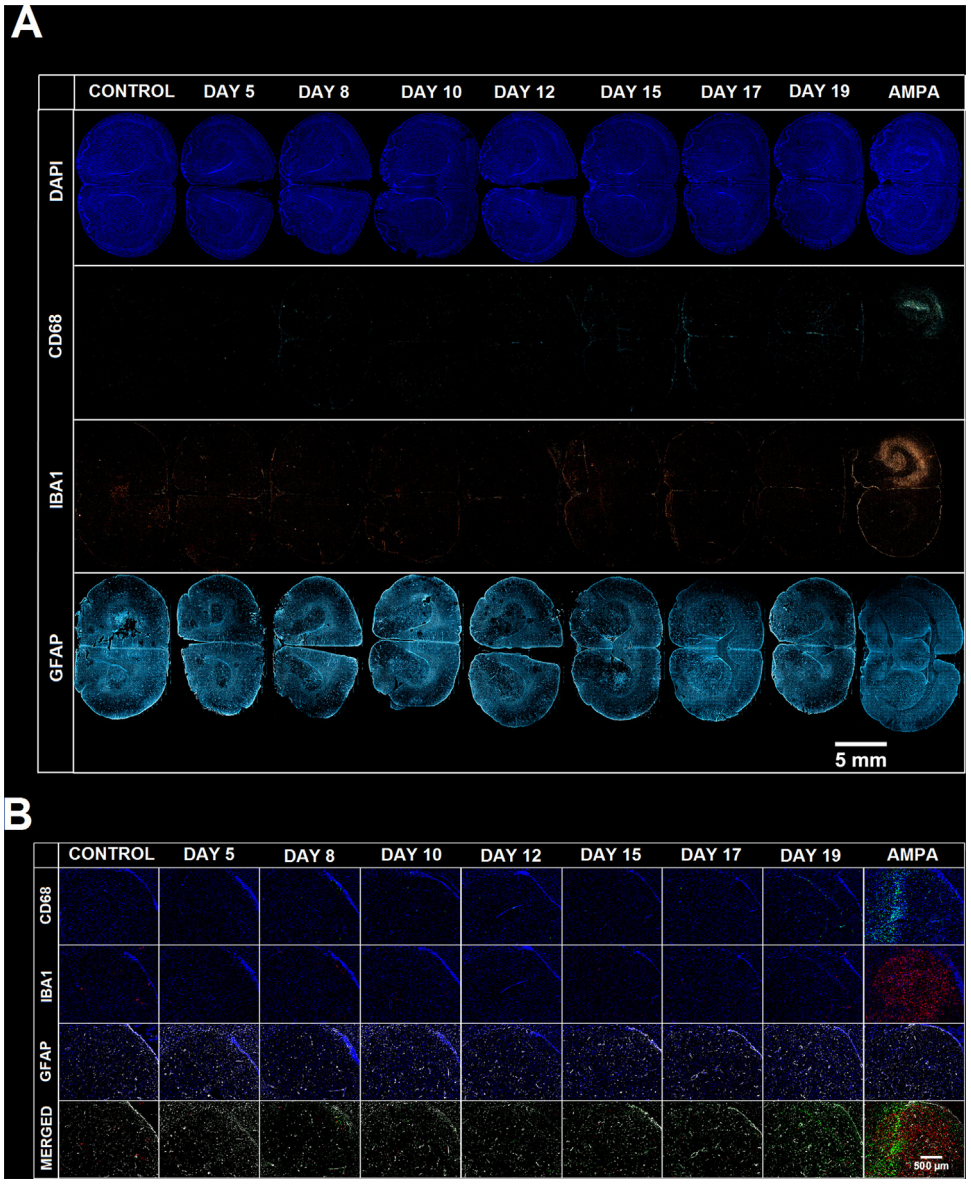

Fig. 5. Immunohistochemical (IHC) analysis of glial markers in a rat model of morphine exposure and withdrawal. Rats were exposed to escalating dose of morphine (Day 5) followed by morphine withdrawal phase (Day 8–Day 19). IHC data were compared to control brain (saline injection instead of morphine) and a validated model of microglial activation (stereotactically injected AMPA). Adjacent brain tissue sections (10 μm) were stained for nucleus (DAPI), activated microglia (CD68,Iba1) and reactive astrocytes (GFAP). Images show fluorescence detection in the whole brain section (A) and in the striatum area (B). A merged image, obtained from adjacent brain sections is shown in B.

stimulation in animal models of stroke or hyperalgesia (Wang et al., 2014b). In our model, we found no significant overexpression of GFAP, Iba1 and CD68 in the rat striatum up to 14 days after morphine withdrawal (Day 19). Using a similar model, Campbell et al. (2013) reported a slight increase in Iba1 positive cells in the striatum 60 h after morphine cessation but other biomarkers of glial activation have not been investigated. In another rodent model, it was reported that morphine withdrawal could induce both the GFAP and the microglial biomarker of activation CD11b expression in the striatum (Hutchinson et al., 2009). However, the control rats used in this study were injected ibudilast, a modulator of glial activation and no comparison to drug-naïve rats was reported.

The absence of detectable activation of glial cells involved in [^{18}F]DPA-714 PET signal (Lavisse et al., 2012) suggests that TSPO PET imaging is not a suitable approach to explore the neuroimmune events induced by morphine exposure, tolerance and withdrawal. It was shown that an increase in inflammatory markers (e.g., cytokines, chemokines) in the CNS may occur without any detectable activation of microglial cells, as demonstrated using Iba1 as a biomarker (Boulay et al., 2015). Moreover, compared to neuroinflammatory processes described in some neurological CNS diseases where [^{18}F]DPA-714 PET imaging is useful, morphine-induced microglial activation may occur at a "subinflammatory" level (Hutchinson and Watkins, 2014). According to this hypothesis, TSPO PET imaging as well as the IHC methodology used in this study may lack sensitivity to detect such phenomena. Alternative imaging methodologies using relevant and highly sensitive biomarkers are therefore needed to non-invasively explore the neuroimmune component of morphine exposure and withdrawal in vivo.

Another possible explanation for the absence of detectable glial activation in our model may be the use of healthy and pathogen-free rats. Environmental factors such as early-life infections have been linked to an increased sensitivity of microglial function (Williamson et al., 2016). Accordingly, long-term changes in microglial function have been associated with an increased risk of drug-induced reinstatement of addiction behavior in adulthood

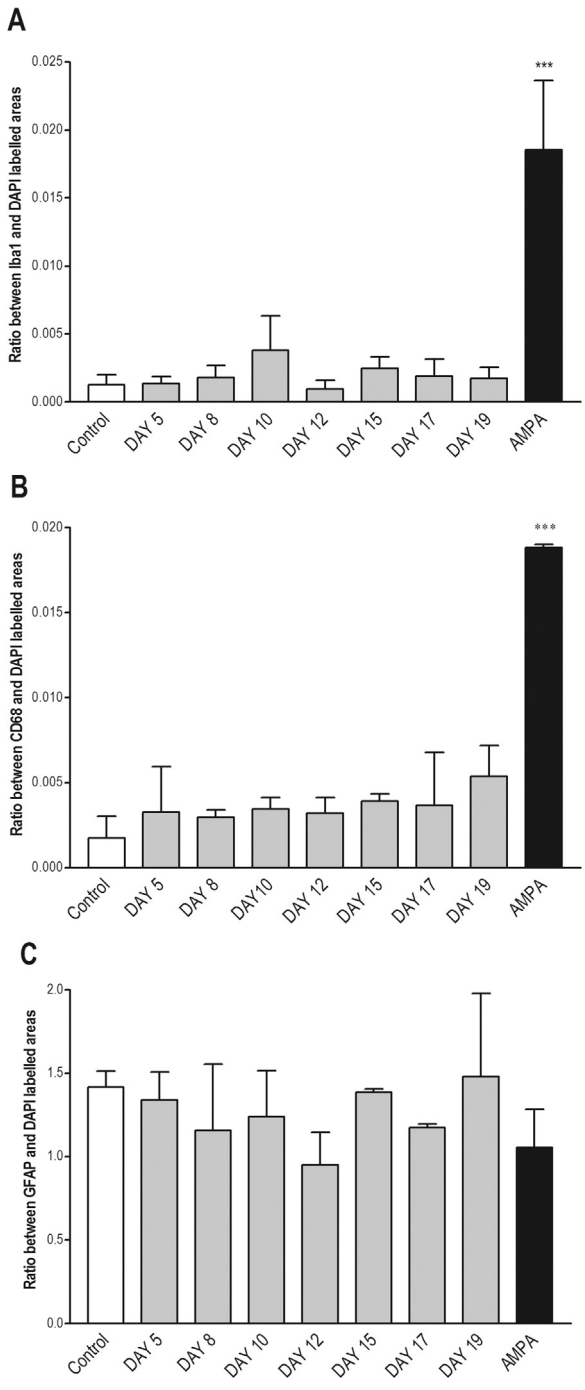

Fig. 6. Expression of glial biomarkers in rat model of morphine exposure and withdrawal. Ratios between tested glial biomarkers of activation and DAPI labelled areas. Saline treated rats are represented as "Control" group (white columns), and the positive control group is represented as "AMPA" group (black columns). Each time point (grey columns) of the glial biomarker expression kinetic after chronic morphine exposure is represented from Day 5 (immediately after the last injection of morphine) to Day 19. The ratio between Iba1 and DAPI labelled areas is shown in A. The ratio between CD68 and DAPI labelled areas is shown in B. The ratio between GFAP and DAPI labelled areas is shown in C. When relevant, *** indicates the statistical difference compared to control with $p < 0.001$.

in rats (Schwarz and Bilbo, 2013). One could thus hypothesize that priming parameters may promote the glial response to morphine exposure and withdrawal in the real-life situation (Auvity et al., 2016).

A growing area of research suggests a role for microglial cell activation in controlling opioid tolerance and dependence in patients. We showed that TSPO PET imaging was not detectably influenced by morphine exposure and withdrawal in healthy rats.

Conflicts of interest

None.

Role of the funding source

This work is supported by a public grant overseen by the French National Research Agency (ANR) as part of the « Investissement d'Avenir » program, through the "Lidex-PIM" project funded by the IDEX Paris-Saclay, ANR-11-IDEX-0003-02. This institution had no further role in study design; in the collection, analysis and interpretation of data; in the writing of the report; and in the decision to submit the paper for publication.

Author contributions

The authors SA, SC and NT were responsible for the study concept and design. SA, SG, CC, WS, RB and BH conducted, analyzed and interpreted the PET experiments. SA, BT and BH conducted, analyzed and interpreted the IHC experiments. BK was in charge with the production of [^{18}F]DPA-714. IB discussed the data and critically revised the manuscript. All authors have approved the submission of the manuscript to Drug and Alcohol Dependence.

Acknowledgement

We thank Thierry Lekieffre for technical assistance.

References

Arlicot, N., Vercouillie, J., Ribeiro, M.-J., Tauber, C., Venel, Y., Baulieu, J.-L., Maia, S., Corcia, P., Stabin, M.G., Reynolds, A., Kassiou, M., Guilloteau, D., 2012. Initial evaluation in healthy humans of [18F]DPA-714, a potential PET biomarker for neuroinflammation. Nucl. Med. Biol. 39, 570–578, http://dx.doi.org/10.1016/j.nucmedbio.2011.10.012.

Auvity, S., Saba, W., Goutal, S., Leroy, C., Buvat, I., Cayla, J., Caillé, F., Bottlaender, M., Cisternino, S., Tournier, N., 2016. Acute morphine exposure increases the brain distribution of [18F]DPA-714, a PET biomarker of glial activation in nonhuman primates. Int. J. Neuropsychopharmacol., http://dx.doi.org/10.1093/ijnp/pyw077.

Boulay, A.-C., Mazeraud, A., Cisternino, S., Saubaméa, B., Mailly, P., Jourdren, L., Blugeon, C., Mignon, V., Smirnova, M., Cavallo, A., Ezan, P., Avé, P., Dingli, F., Loew, D., Vieira, P., Chrétien, F., Cohen-Salmon, M., 2015. Immune quiescence of the brain is set by astroglial connexin 43. J. Neurosci. 35, 4427–4439, http://dx.doi.org/10.1523/JNEUROSCI.2575-14.2015.

Campbell, L.A., Avdoshina, V., Rozzi, S., Mocchetti, I., 2013. CCL5 and cytokine expression in the rat brain: differential modulation by chronic morphine and morphine withdrawal. Brain Behav. Immun. 34, 130–140, http://dx.doi.org/10.1016/j.bbi.2013.08.006.

Chauveau, F., Van Camp, N., Dollé, F., Kuhnast, B., Hinnen, F., Damont, A., Boutin, H., James, M., Kassiou, M., Tavitian, B., 2009. Comparative evaluation of the translocator protein radioligands 11C-DPA-713, 18F-DPA-714, and 11C-PK11195 in a rat model of acute neuroinflammation. J. Nucl. Med. 50, 468–476, http://dx.doi.org/10.2967/jnumed.108.058669.

Coller, J.K., Hutchinson, M.R., 2012. Implications of central immune signaling caused by drugs of abuse: mechanisms, mediators and new therapeutic approaches for prediction and treatment of drug dependence. Pharmacol. Ther. 134, 219–245, http://dx.doi.org/10.1016/j.pharmthera.2012.01.008.

Cooper, Z.D., Johnson, K.W., Pavlicova, M., Glass, A., Vosburg, S.K., Sullivan, M.A., Manubay, J.M., Martinez, D.M., Jones, J.D., Saccone, P.A., Comer, S.D., 2015. The effects of ibudilast, a glial activation inhibitor, on opioid withdrawal symptoms in opioid-dependent volunteers. Addict. Biol., http://dx.doi.org/10.1111/adb.12261.

Corcia, P., Tauber, C., Vercoullie, J., Arlicot, N., Prunier, C., Praline, J., Nicolas, G., Venel, Y., Hommet, C., Baulieu, J.-L., Cottier, J.-P., Roussel, C., Kassiou, M., Guilloteau, D., Ribeiro, M.-J., 2012. Molecular imaging of microglial activation in amyotrophic lateral sclerosis. PLoS One 7, e52941, http://dx.doi.org/10.1371/journal.pone.0052941.

Damont, A., Hinnen, F., Kuhnast, B., Schöllhorn-Peyronneau, M.-A., James, M., Luus, C., Tavitian, B., Kassiou, M., Dollé, F., 2008. Radiosynthesis of [18F]DPA-714, a selective radioligand for imaging the translocator protein (18 kDa) with PET. J. Label. Compd. Radiopharm. 51, 286–292, http://dx.doi.org/10.1002/jlcr.1523.

Desjardins, S., Belkai, E., Crete, D., Cordonnier, L., Scherrmann, J.-M., Noble, F., Marie-Claire, C., 2008. Effects of chronic morphine and morphine withdrawal on gene expression in rat peripheral blood mononuclear cells. Neuropharmacology 55, 1347–1354, http://dx.doi.org/10.1016/j.neuropharm.2008.08.027.

Harhausen, D., Sudmann, V., Khojasteh, U., Müller, J., Zille, M., Graham, K., Thiele, A., Dyrks, T., Dirnagl, U., Wunder, A., 2013. Specific imaging of inflammation with the 18 kDa translocator protein ligand DPA-714 in animal models of epilepsy and stroke. PLoS One 8, e69529, http://dx.doi.org/10.1371/journal.pone.0069529.

Hutchinson, M.R., Watkins, L.R., 2014. Why is neuroimmunopharmacology crucial for the future of addiction research? Neuropharmacology 76 (Pt B), 218–227, http://dx.doi.org/10.1016/j.neuropharm.2013.05.039.

Hutchinson, M.R., Bland, S.T., Johnson, K.W., Rice, K.C., Maier, S.F., Watkins, L.R., 2007. Opioid-induced glial activation: mechanisms of activation and implications for opioid analgesia, dependence, and reward. ScientificWorldJournal 7, 98–111, http://dx.doi.org/10.1100/tsw.2007.230.

Hutchinson, M.R., Zhang, Y., Brown, K., Coats, B.D., Shridhar, M., Sholar, P.W., Patel, S.J., Crysdale, N.Y., Harrison, J.A., Maier, S.F., Rice, K.C., Watkins, L.R., 2008. Non-stereoselective reversal of neuropathic pain by naloxone and naltrexone: involvement of toll-like receptor 4 (TLR4). Eur. J. Neurosci. 28, 20–29, http://dx.doi.org/10.1111/j.1460-9568.2008.06321.x.

Hutchinson, M.R., Lewis, S.S., Coats, B.D., Skyba, D.A., Crysdale, N.Y., Berkelhammer, D.L., Brzeski, A., Northcutt, A., Vietz, C.M., Judd, C.M., Maier, S.F., Watkins, L.R., Johnson, K.W., 2009. Reduction of opioid withdrawal and potentiation of acute opioid analgesia by systemic AV411 (ibudilast). Brain Behav. Immun. 23, 240–250, http://dx.doi.org/10.1016/j.bbi.2008.09.012.

Hutchinson, M.R., Shavit, Y., Grace, P.M., Rice, K.C., Maier, S.F., Watkins, L.R., 2011. Exploring the neuroimmunopharmacology of opioids: an integrative review of mechanisms of central immune signaling and their implications for opioid analgesia. Pharmacol. Rev. 63, 772–810, http://dx.doi.org/10.1124/pr.110.004135.

Hutchinson, M.R., Northcutt, A.L., Hiranita, T., Wang, X., Lewis, S.S., Thomas, J., van Steeg, K., Kopajtic, T.A., Loram, L.C., Sfregola, C., Galer, E., Miles, N.E., Bland, S.T., Amat, J., Rozeske, R.R., Maslanik, T., Chapman, T.R., Strand, K.A., Fleshner, M., Bachtell, R.K., Somogyi, A.A., Yin, H., Katz, J.L., Rice, K.C., Maier, S.F., Watkins, L.R., 2012. Opioid activation of toll-like receptor 4 contributes to drug reinforcement. J. Neurosci. 32, 11187–11200, http://dx.doi.org/10.1523/JNEUROSCI.0684-12.2012.

Johnson, J.L., Kwok, Y.H., Sumracki, N.M., Swift, J.E., Hutchinson, M.R., Johnson, K., Williams, D.B., Tuke, J., Rolan, P.E., 2015. Glial attenuation with ibudilast in the treatment of medication overuse headache: a double-blind, randomized, placebo-controlled pilot trial of efficacy and safety. Headache, http://dx.doi.org/10.1111/head.12655.

Koob, G.F., Volkow, N.D., 2010. Neurocircuitry of addiction. Neuropsychopharmacology 35, 217–238, http://dx.doi.org/10.1038/npp.2009.110.

Kuhnast, B., Damont, A., Hinnen, F., Catarina, T., Demphel, S., Le Helleix, S., Coulon, C., Goutal, S., Gervais, P., Dollé, F., 2012. [18F]DPA-714, [18F]PBR111 and [18F]FEDAA1106—selective radioligands for imaging TSPO 18 kDa with PET: automated radiosynthesis on a TRACERLAb FX-FN synthesizer and quality controls. Appl. Radiat. Isot. 70, 489–497, http://dx.doi.org/10.1016/j.apradiso.2011.10.015.

Lavisse, S., Guillermier, M., Hérard, A.-S., Petit, F., Delahaye, M., Van Camp, N., Ben Haim, L., Lebon, V., Remy, P., Dollé, F., Delzescaux, T., Bonvento, G., Hantraye, P., Escartin, C., 2012. Reactive astrocytes overexpress TSPO and are detected by TSPO positron emission tomography imaging. J. Neurosci. 32, 10809–10818, http://dx.doi.org/10.1523/JNEUROSCI.1487-12.2012.

Lavisse, S., García-Lorenzo, D., Peyronneau, M.-A., Bodini, B., Thiriez, C., Kuhnast, B., Comtat, C., Remy, P., Stankoff, B., Bottlaender, M., 2015. Optimized quantification of translocator protein radioligand ^{18}F-DPA-714 uptake in the brain of genotyped healthy volunteers. J. Nucl. Med. 56, 1048–1054, http://dx.doi.org/10.2967/jnumed.115.156083.

Loram, L.C., Grace, P.M., Strand, K.A., Taylor, F.R., Ellis, A., Berkelhammer, D., Bowlin, M., Skarda, B., Maier, S.F., Watkins, L.R., 2012. Prior exposure to repeated morphine potentiates mechanical allodynia induced by peripheral inflammation and neuropathy. Brain Behav. Immun. 26, 1256–1264, http://dx.doi.org/10.1016/j.bbi.2012.08.003.

Mosser, D.M., Edwards, J.P., 2008. Exploring the full spectrum of macrophage activation. Nat. Rev. Immunol. 8, 958–969, http://dx.doi.org/10.1038/nri2448.

Nielsen, D.A., Kreek, M.J., 2012. Common and specific liability to addiction: approaches to association studies of opioid addiction. Drug Alcohol Depend. 123 (Suppl. 1), S33–41, http://dx.doi.org/10.1016/j.drugalcdep.2012.03.026.

Nutt, D.J., Lingford-Hughes, A., Erritzoe, D., Stokes, P.R.A., 2015. The dopamine theory of addiction: 40 years of highs and lows. Nat. Rev. Neurosci. 16, 305–312, http://dx.doi.org/10.1038/nrn3939.

Perry, V.H., Nicoll, J.A.R., Holmes, C., 2010. Microglia in neurodegenerative disease. Nat. Rev. Neurol. 6, 193–201, http://dx.doi.org/10.1038/nrneurol.2010.17.

Peyronneau, M.-A., Saba, W., Goutal, S., Damont, A., Dollé, F., Kassiou, M., Bottlaender, M., Valette, H., 2013. Metabolism and quantification of [(18)F]DPA-714, a new TSPO positron emission tomography radioligand. Drug Metab. Dispos. 41, 122–131, http://dx.doi.org/10.1124/dmd.112.046342.

Qiu, S., Feng, Y., LeSage, G., Zhang, Y., Stuart, C., He, L., Li, Y., Caudle, Y., Peng, Y., Yin, D., 2015. Chronic morphine-induced microRNA-124 promotes microglial immunosuppression by modulating P65 and TRAF6. J. Immunol. 194, 1021–1030, http://dx.doi.org/10.4049/jimmunol.1400106.

Roy, S., Ninkovic, J., Banerjee, S., Charboneau, R.G., Das, S., Dutta, R., Kirchner, V.A., Koodie, L., Ma, J., Meng, J., Barke, R.A., 2011. Opioid drug abuse and modulation of immune function: consequences in the susceptibility to opportunistic infections. J. Neuroimmune Pharmacol. 6, 442–465, http://dx.doi.org/10.1007/s11481-011-9292-5.

Saijo, K., Glass, C.K., 2011. Microglial cell origin and phenotypes in health and disease. Nat. Rev. Immunol. 11, 775–787, http://dx.doi.org/10.1038/nri3086.

Schiffer, W.K., Mirrione, M.M., Biegon, A., Alexoff, D.L., Patel, V., Dewey, S.L., 2006. Serial microPET measures of the metabolic reaction to a microdialysis probe implant. J. Neurosci. Methods 155, 272–284, http://dx.doi.org/10.1016/j.jneumeth.2006.01.027.

Schwarz, J.M., Bilbo, S.D., 2013. Adolescent morphine exposure affects long-term microglial function and later-life relapse liability in a model of addiction. J. Neurosci. 33, 961–971, http://dx.doi.org/10.1523/JNEUROSCI.2516-12.2013.

Song, P., Zhao, Z.Q., 2001. The involvement of glial cells in the development of morphine tolerance. Neurosci. Res. 39, 281–286.

Trescot, A.M., Datta, S., Lee, M., Hansen, H., 2008. Opioid pharmacology. Pain Physician 11, S133–153.

Wang, Y., Yue, X., Kiesewetter, D.O., Niu, G., Teng, G., Chen, X., 2014a. PET imaging of neuroinflammation in a rat traumatic brain injury model with radiolabeled TSPO ligand DPA-714. Eur. J. Nucl. Med. Mol. Imaging 41, 1440–1449, http://dx.doi.org/10.1007/s00259-014-2727-5.

Wang, Y., Yue, X., Kiesewetter, D.O., Wang, Z., Lu, J., Niu, G., Teng, G., Chen, X., 2014b. [(18)F]DPA-714 PET imaging of AMD3100 treatment in a mouse model of stroke. Mol. Pharmacol. 11, 3463–3470, http://dx.doi.org/10.1021/mp500234d.

Watkins, L.R., Hutchinson, M.R., Johnston, I.N., Maier, S.F., 2005. Glia: novel counter-regulators of opioid analgesia. Trends Neurosci. 28, 661–669, http://dx.doi.org/10.1016/j.tins.2005.10.001.

Watkins, L.R., Hutchinson, M.R., Rice, K.C., Maier, S.F., 2009. The toll of opioid-induced glial activation: improving the clinical efficacy of opioids by targeting glia. Trends Pharmacol. Sci. 30, 581–591, http://dx.doi.org/10.1016/j.tips.2009.08.002.

Williamson, L.L., McKenney, E.A., Holzknecht, Z.E., Belliveau, C., Rawls, J.F., Poulton, S., Parker, W., Bilbo, S.D., 2016. Got worms? Perinatal exposure to helminths prevents persistent immune sensitization and cognitive dysfunction induced by early-life infection. Brain. Behav. Immun. 51, 14–28, http://dx.doi.org/10.1016/j.bbi.2015.07.006.